Application of the Beltrami-Michell method for stress prediction

Fernando T. B. Andrade, Lourenildo W. B. Leite, UFPA, Brazil

Abstract

This work is developed for modeling of stresses, with a focus on low and high-pressure zones in a sedimentary basin, that relate to a reservoir and petroleum generator zones. The numerical experiment is a demonstration of the principle that the first stress invariant controls the geology described as a process of the mechanics of solids under the influence of gravity attraction. The physical problem is constructed as a boundary value problem (BVP) involving the Beltrami-Michell equation with Dirichlet conditions, where we use the method of Green's function represented by a Fourier series for the solution of the BVP. The boundary conditions are given by stress distributions along the border of the target volume. Once the rock pressure distribution is obtained and boundary conditions are defined, the solution of the BVP allows the calculation of the stress components distribution (normal and tangential) inside the target volume. The relationship between rock pressure and stress components is established by the Beltrami-Michell problem, which has the form of a Poisson equation. The proposed method was applied in target zones containing possible reservoirs, where we used the Beltrami-Michell equation to calculate stress components variations in the region of interest.

Introduction

The present stress modeling is related to the geological scale, and not to the local engineering scale that acts during drilling. Therefore, the interpretation is centered on identifying low and high-pressure zones in the sedimentary basin, to map and/or extend a potential productive zone. The main motivation is that low and high-pressure zones act as natural pumps for fluids (water, oil, and gas), that tend to accumulate in the low-pressure zones.

The work is motivated by the natural description of a sedimentary basin based on the mechanics of solids under gravity loading, where the effect is the only stress agent in the sedimentary basin. This modeling is a data-driven process, where the necessary information is seismic data: distribution of P and S wave velocities, $V_p(\mathbf{x})$, $V_s(\mathbf{x})$ and density, $\rho(\mathbf{x})$. From the geomechanical principle, a reservoir corresponds to a low-pressure zone capped by a high-pressure zone, and controlled by the $\gamma = \frac{V_s(\mathbf{x})}{V_p(\mathbf{x})}$ ratio contrast across the interface of these zones. Besides the mechanical conjecture, the principles of the petroleum geology system are also applied.

It is described in the specialized literature, that the pressure variation in the subsurface is directly related to the first stress invariant. Therefore, the method is to predict the stress tensor components (normal and tangential) from the first stress invariant (defined as the average of the normal stresses, and called "rock pressure"). The problem is structured as a BVP for the Beltrami-Michell equation under Dirichlet conditions and applied in a specific target zone. The boundary conditions for the target zones are defined from the stress components values, based on the mechanics of solids under gravity loading.

The major part of the study was to validate the numerical solution of the Beltrami-Michell equation for a geological-geophysical model, where the geological complexity poses a challenge in predicting stress components in a target zone. The Beltrami-Michell equation considers a constant value for the Poisson's ratio, which is only realistic as an average for a complex geological media. Therefore, we investigate how gradients in the elastic parameters can affect the solution for the stress components in a target zone.

Method

Equilibrium Equations

The modeling considers the vertical gravity loading as a stress-causing agent in the sedimentary basin, without considering lateral tectonic forces. Therefore, the system of equilibrium equations is defined as follows:

$$\frac{\partial \sigma_{xx}}{\partial x} + \frac{\partial \sigma_{xy}}{\partial y} + \frac{\partial \sigma_{xz}}{\partial z} = 0, \tag{1}$$

$$\frac{\partial \sigma_{yx}}{\partial x} + \frac{\partial \sigma_{yy}}{\partial y} + \frac{\partial \sigma_{yz}}{\partial z} = 0, \tag{2}$$

$$\frac{\partial \sigma_{zx}}{\partial x} + \frac{\partial \sigma_{zy}}{\partial y} + \frac{\partial \sigma_{zz}}{\partial z} = \rho g, \tag{3}$$

where ρ is the bulk density and g is the gravity acceleration.

Linear Hooke's Law

For an isotropic medium, the linear relationship between stress σ_{ij} and strain ε_{ij} at a certain point is given by Hooke's law:

$$\sigma_{ij} = \lambda \theta \delta_{ij} + 2\mu \varepsilon_{ij}, \tag{4}$$

where μ and λ are the Lame's elastic parameters, θ the dilation, δ_{ij} the Kronecker delta, ε_{ij} the strain tensor.

The normal vertical stress is defined as the overburden weight of the rock formation and fluids down to the reference point. From equilibrium equations (1), the normal vertical stress is defined by:

$$\sigma_{zz}(z) = g \int_{z_0}^{z} \rho(z) dz, \tag{5}$$

where ρ is the bulk density, $z_0 = 0$ is the initial depth, z is the depth point of interest, and g is the gravity acceleration, considered constant in the interval (z_0, z).

Using Hooke's law for the isotropic medium (4), and assuming that each subsurface element is confined, we consider the absence of lateral deformations ($\varepsilon_{xx} = \varepsilon_{yy} = 0$). Consequently, the horizontal normal stresses σ_{xx} and σ_{yy} are written as a function of the normal vertical stress σ_{zz}:

$$\sigma_{xx} = \sigma_{yy} = (1 - 2\gamma^2)\sigma_{zz}, \tag{6}$$

where γ is the ratio of the seismic velocities V_p and V_s, functions of density and Lamé elastic parameters

$$\gamma = \frac{V_\mathrm{s}}{V_\mathrm{p}}, \quad V_\mathrm{s} = \sqrt{\frac{\mu}{\rho}}, \quad V_\mathrm{p} = \sqrt{\frac{\lambda + 2\mu}{\rho}}. \tag{7}$$

A formal measure, named rock pressure, P_r, is defined as a simple average of the normal stresses in the form:

$$P_r = \frac{1}{3}(\sigma_{xx} + \sigma_{yy} + \sigma_{zz}). \tag{8}$$

The stress is non-hydrostatic, and an important symmetry condition in the model is $\sigma_{xx} = \sigma_{yy}$. For modeling a real complex case, we can consider that σ_{xx}, σ_{yy}, and σ_{zz} are different from each other.

The Beltrami-Michell Equation

The Beltrami-Michell equation form a set of compatibility relations that describes the distribution of stress in a solid medium as a boundary value problem (Sadd, 2005; Saada, 1974):

$$\nabla^2 \sigma_{ij} = -\frac{3}{1+\nu}\frac{\partial^2 P_r}{\partial x_i \partial x_j} - \frac{\nu}{1-\nu}\delta_{ij}\nabla\cdot\mathbf{F} - \left(\frac{\partial F_i}{\partial x_j} + \frac{\partial F_j}{\partial x_i}\right), \tag{9}$$

where σ_{ij} is the stress tensor components, P_r is the rock pressure, ν is the Poisson's ratio, $\mathbf{F}$ is the gravity internal force vector and δ_{ij} is the Kronecker delta. Adding the equations corresponding to the normal stresses, we obtain an important relationship between body forces $\mathbf{F}$ and the rock pressure P_r:

$$\nabla\cdot\mathbf{F} = -\frac{3(1-\nu)}{1+\nu}\nabla^2 P_r. \tag{10}$$

The Beltrami-Michell partial differential equation establishes a relationship between the rock pressure, P_r, and the stress field, σ_{ij}. Therefore, once the rock pressure field is known, the stress components can be obtained for a specific region of interest by solving the differential equations (9) as a boundary value problem.

The elastic parameter ν is the main elastic parameter that affects the Beltrami-Michell equation. This parameter is limited to the range $-1 < \nu < 0.5$ for isotropic materials, with typical engineering values between $0.2 < \nu < 0.5$ (Novacky, 1975; Boresi and Schmidt, 1965). In the Beltrami-Michell equation, the Poisson's ratio is constant in its application volume. A variation in this parameter causes deviations in the solution for the stress components σ_{ij}.

Boundary Value Problem and Solution Decomposition

The BVP associated with the Beltrami-Michell equation consists of finding a solution within a domain V (target-zone) subject to boundary conditions in S. Therefore, the Dirichlet boundary value problem (DBVP) applied to the Beltrami-Michell equation is formulated as:

$$\begin{aligned} \nabla^2\sigma_{ij}(\mathbf{x}) &= f_{ij}(\mathbf{x}), \quad (\text{in } V), \\ \sigma_{ij}(\mathbf{x}) &= b_{ij}(\mathbf{x}), \quad (\text{on } S), \end{aligned} \tag{11}$$

where $\sigma_{ij}(\mathbf{x})$ is the stress component field, f_{ij} is the right-hand side of the Beltrami-Michell equation and $b_{ij}(\mathbf{x})$ specifies the solution value at the boundary S, as illustrated in the Figure (1).

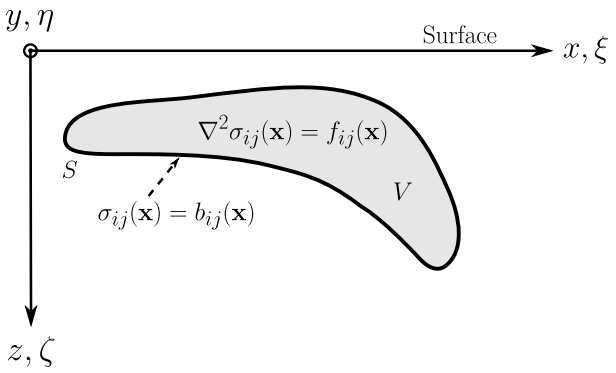

Figure 1: Representation of the Dirichlet boundary value problem (DBVP) applied to the Beltrami-Michell equation. The interior of the closed volume (in gray) is represented by V, and its boundary by S. The function $b_{ij}(\mathbf{x})$ defines the boundary conditions imposed on the stress component field $\sigma_{ij}(\mathbf{x})$.

The solution of the BVP (11) can be simplified by decomposing it into two sub-problems:

1. Homogeneous sub-problem, defined by

$$\begin{aligned} \nabla^2\sigma_{ij}^{(\mathrm{h})}(\mathbf{x}) &= 0, \quad (\text{in } V), \\ \sigma_{ij}^{(\mathrm{h})}(\mathbf{x}) &= b_{ij}(\mathbf{x}), \quad (\text{on } S), \end{aligned} \tag{12}$$

2. Nonhomogeneous or particular sub-problem, defined by

$$\begin{aligned} \nabla^2\sigma_{ij}^{(\mathrm{p})}(\mathbf{x}) &= f_{ij}(\mathbf{x}), \quad (\text{in } V), \\ \sigma_{ij}^{(\mathrm{p})}(\mathbf{x}) &= 0, \quad (\text{on } S). \end{aligned} \tag{13}$$

Therefore, the complete solution $\sigma_{ij}^{(\mathrm{c})}$ is obtained using the use superposition to combine the separate solutions:

$$\sigma_{ij}^{(\mathrm{c})}(\mathbf{x}) = \sigma_{ij}^{(\mathrm{h})}(\mathbf{x}) + \sigma_{ij}^{(\mathrm{p})}(\mathbf{x}), \tag{14}$$

where $\sigma_{ij}^{(\mathrm{h})}$ is the homogeneous solution and $\sigma_{ij}^{(\mathrm{p})}$ is the particular solution.

Homogeneous Solution in a Rectangular Target Zone

This sub-problem aims to determine a solution for Laplace's equation in a domain defined by a rectangle of length L and height H subject to prescribed values on the boundary. Thus, the desired solution is a function $\varphi(x,z)$ that satisfies Laplace's differential equation and the Dirichlet boundary conditions in the Figure 2.

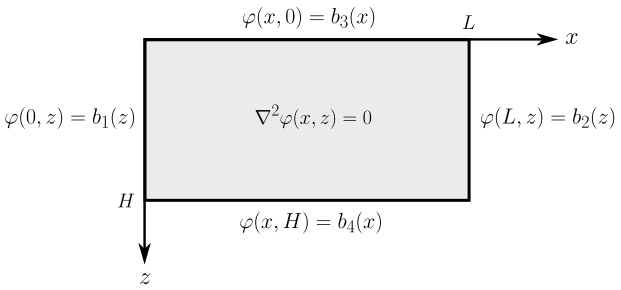

Figure 2: Boundary value problem for Laplace's equation in a rectangle with Dirichlet conditions.

The solution $\varphi(x,z)$ can be written as a Fourier series in the form:

$$\varphi(x,z) = \sum_{n=1}^{\infty} A_n \frac{\sinh[p_n(L-x)]}{\sinh(p_nL)} \sin(p_nz) + \sum_{n=1}^{\infty} B_n \frac{\sinh(p_nx)}{\sinh(p_nL)} \sin(p_nz) + \sum_{n=1}^{\infty} C_n \frac{\sinh[q_n(H-z)]}{\sinh(q_nH)} \sin(q_nx) + \sum_{n=1}^{\infty} D_n \frac{\sinh(q_nz)}{\sinh(q_nH)} \sin(q_nx), \tag{15}$$

where the Fourier coefficients A_n, B_n, C_n and D_n are calculated by

$$A_n = \frac{2}{H}\int_0^H b_1(z)\sin(p_nz)\,dz, \quad B_n = \frac{2}{H}\int_0^H b_2(z)\sin(p_nz)\,dz,$$
$$C_n = \frac{2}{L}\int_0^L b_3(x)\sin(q_nx)\,dx, \quad D_n = \frac{2}{L}\int_0^L b_4(x)\sin(q_nx)\,dx,$$

and the parameters p_n and q_n are the angular frequencies given by

$$p_n = \frac{n\pi}{H}, \quad q_n = \frac{n\pi}{L}.$$

Particular Solution in a Rectangular Target Zone

This sub-problem consists to find a solution for Poisson's equation in a domain defined by a rectangle subject to boundary values. The desired solution is a function $\varphi(x,z)$ defined on the rectangular domain governed by Poisson's equation and the boundary conditions shown in Figure 3.

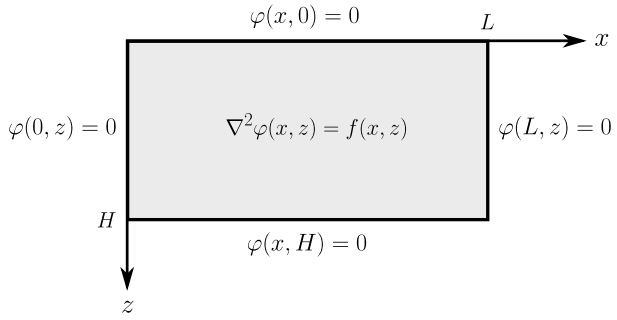

Figure 3: BVP for the Poisson's equation in a rectangle with Dirichlet conditions.

In this case, the solution $\varphi(x,z)$ is given by:

$$\varphi(x,z) = \int_0^L \int_0^H f(\xi,\zeta)G(x,z\,|\,\xi,\zeta)d\zeta d\xi, \tag{16}$$

where G is the Green's function for the Laplacian operator (∇^2), given by Fourier series (Polyanin, 2016)

$$G(x,z\,|\,\xi,\zeta) = \frac{2}{L}\sum_{n=1}^{\infty} \frac{\sin(p_nx)\sin(p_n\xi)}{p_n\sinh(p_nH)} E_n(z,\zeta), \tag{17}$$

where

$$E_n(z,\zeta) = \begin{cases} \sinh(p_n\zeta)\sinh[p_n(H-z)] & \text{for } H \geq z > \zeta \geq 0, \\ \sinh(p_nz)\sinh[p_n(H-\zeta)] & \text{for } H \geq \zeta > z \geq 0. \end{cases}$$

and the parameter p_n is the angular frequency given by

$$p_n = \frac{n\pi}{H}.$$

Results

This numerical experiment was the calculation of the stress components σ_{ij} in a rectangular target zone containing a reservoir in the Marmousi geological basin (Figure 4). The rock pressure field is calculated using the velocities and density available distributions. The purpose of this experiment was to analyze the stress distribution along a reservoir zone in a plausible geological context.

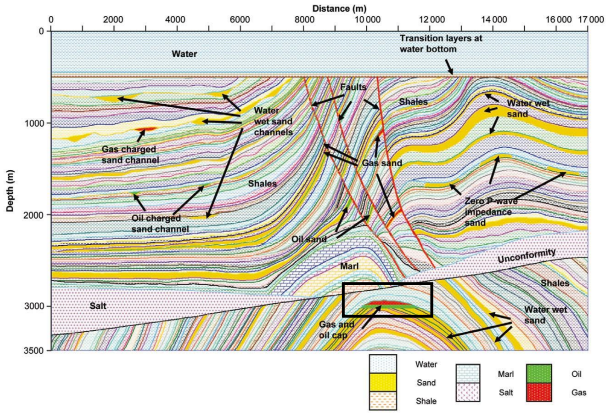

Figure 4: Structural elements, formations, and lithologies of the Marmousi basin (Martin et al., 2006). The black rectangle represents the selected target zone. The vertical exaggeration is of the order 4:1.

Rock Pressure and Target Zone Selection

Figure (4) displays the selected target zone, which includes the anticline structure containing the gas and oil cap, located around 3000 meters in depth and between 10000 and 12000 meters in horizontal distance. Figures (5) and (6) show, respectively, the distribution of rock pressure and the selected target zone used in the calculating of stress components.

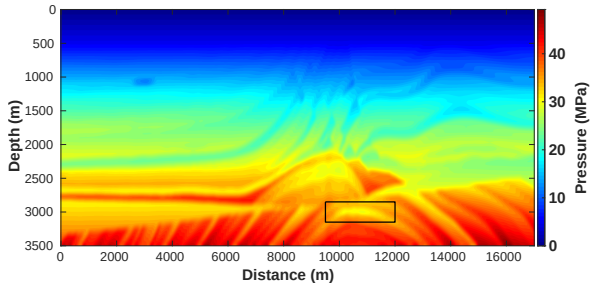

Figure 5: The rock pressure distribution, $P_r(x,z)$, for the Marmousi model. The black rectangle represents the selected target zone used in the application of the Beltrami-Michell problem.

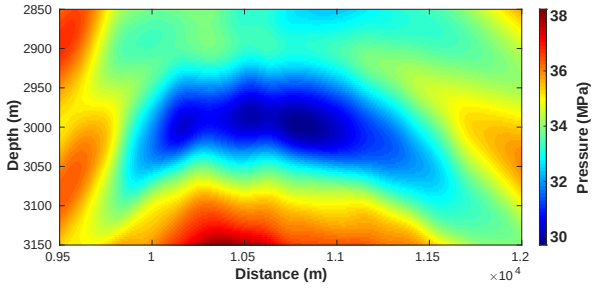

Figure 6: Target selected from figure 5.

Results of the Beltrami-Michell Problem

Figure 7 shows the complete solution for the normal vertical stress, $\sigma_{zz}^{(c)}$. This solution maps a low-stress zone at the top of the anticline. Figure 8 shows the normal vertical stress from direct modeling [equation (5)] and presents a smooth and increasing behavior with depth, with a smooth horizontal variation. The deviation between direct modeling and the Beltrami-Michell method is close to 15% for the vertical stress component (Figure 9).

Figure 10 shows the complete solution for the normal horizontal stress, $\sigma_{xx}^{(c)}$. This solution maps low stress at the top of the anticline, highlighting the reservoir shape. Figure 17 shows the normal horizontal stress from direct modeling [equation (6)] and maps the low-stress zone and shape of the anticline structure. The deviation between direct modeling and the Beltrami-Michell method is close to 30% for the horizontal stress component (Figure 12).

For the shear component, the complete solution $\sigma_{xz}^{(c)}$ [figure 13] presents low shear stress at the top of the anticline, and high values on the sides. This indicates a larger tendency for fracturing in regions further away from the reservoir.

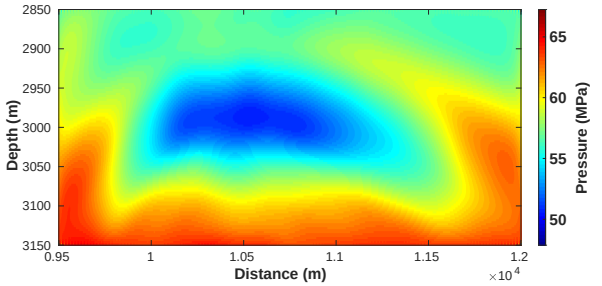

Figure 7: The complete solution for the normal vertical stress, $\sigma_{zz}^{(c)} = \sigma_{zz}^{(p)} + \sigma_{zz}^{(h)}$. The Poisson's coefficient used was $\nu = 0.35$.

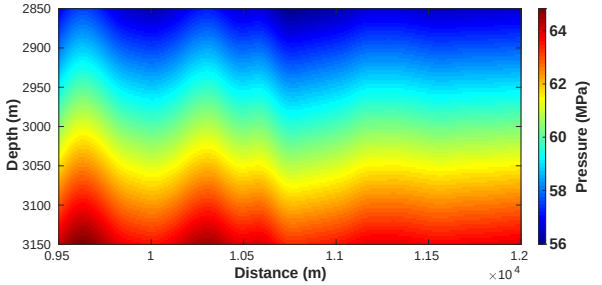

Figure 8: Normal vertical stress calculated by direct modeling.

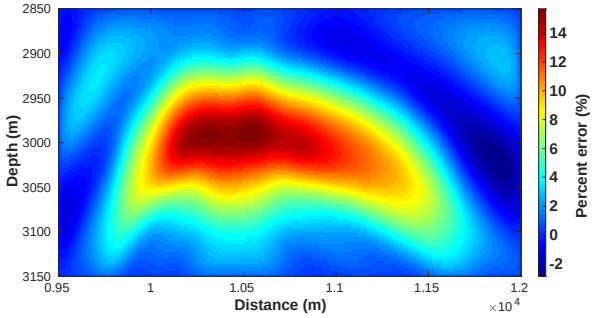

Figure 9: Percentual deviation between the direct modeling and the Beltrami-Michell method for the normal vertical stress.

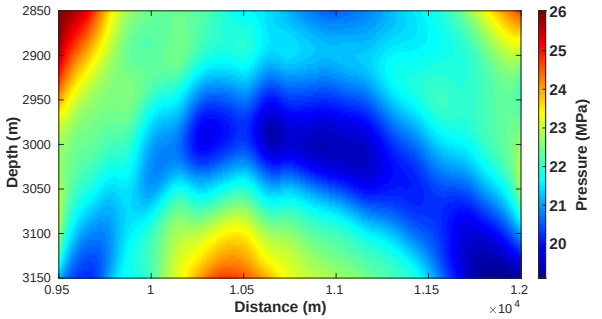

Figure 10: The complete solution for the horizontal normal stress $\sigma_{xx}^{(c)} = \sigma_{xx}^{(p)} + \sigma_{xx}^{(h)}$. The Poisson's coefficient used was $\nu = 0.35$.

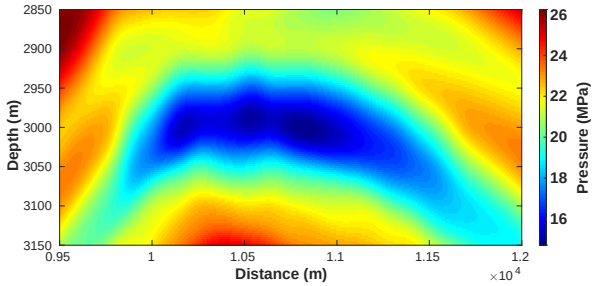

Figure 11: Normal horizontal stress calculated by direct modeling.

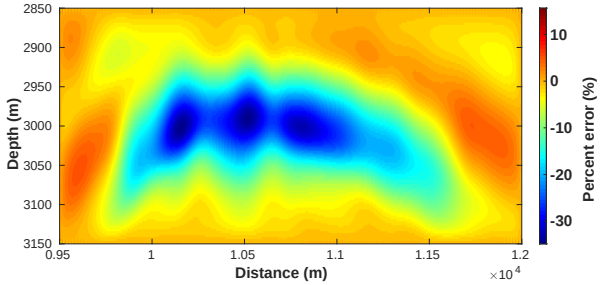

Figure 12: Percentual deviation between the direct modeling and the Beltrami-Michell method for the normal horizontal stress.

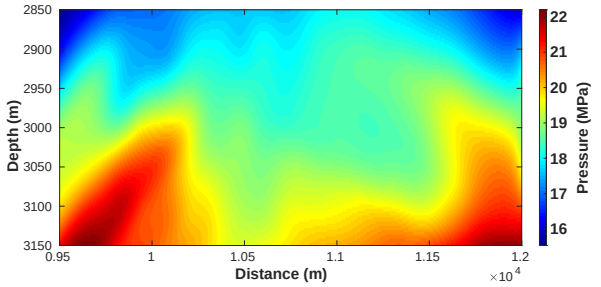

Figure 13: The complete solution for the shear stress $\sigma_{xz}^{(c)} = \sigma_{xz}^{(p)} + \sigma_{xz}^{(h)}$.

Correction of deviations in the Beltrami-Michell solution

The variation of the Poisson's coefficient in the target zone generates deviations in the solutions of the Beltrami-Michell equations. However, the complete solutions $\sigma_{zz}^{(c)}$ and $\sigma_{xx}^{(c)}$ reconstruct the rock pressure distribution very similar to the original input data. This observation indicates that the deviations present in the horizontal and vertical components are compensated when we calculate the rock pressure using the complete solutions. We can express this observation by splitting the complete solution in the following way:

$$P_r^{(c)} = \frac{2\sigma_{xx}^{(c)} + \sigma_{zz}^{(c)}}{3}, \tag{18}$$

$$P_r^{(c)} = \frac{2}{3}\left[\sigma_{xx}^{(h)} + \sigma_{xx}^{(p)}\right] + \frac{1}{3}\left[\sigma_{zz}^{(h)} + \sigma_{zz}^{(p)}\right]. \tag{19}$$

From the comparison between the vertical stress component obtained in the direct modeling, σ_{zz}, and the homogeneous solution $\sigma_{zz}^{(h)}$ (Figures 14 and 15), we observe that this component presents a harmonic behavior, being better described only by the homogeneous solution:

$$\sigma_{zz}^{(c)} \approx \sigma_{zz}^{(h)}. \tag{20}$$

Considering $\sigma_{zz}^{(c)}$ to be harmonic and using the rock pressure equation (19), the deviation in the $\sigma_{xx}^{(c)}$ component is compensated for in the following way:

$$\sigma_{xx}^{(c)} \approx \sigma_{xx}^{(h)} + \sigma_{xx}^{(p)} + \frac{1}{2}\sigma_{zz}^{(p)}, \tag{21}$$

where the presence of the particular term $\frac{1}{2}\sigma_{zz}^{(p)}$ corrects the calculation of the horizontal stress (Figures 16 and 17).

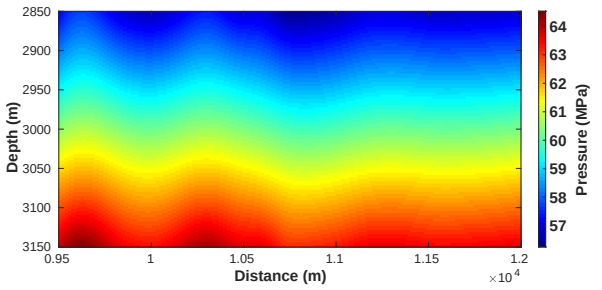

Figure 14: The homogeneous solution for the vertical normal stress $\sigma_{zz}^{(h)}$.

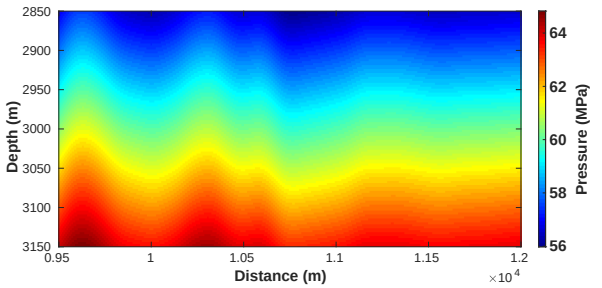

Figure 15: Normal vertical stress calculated by direct modeling.

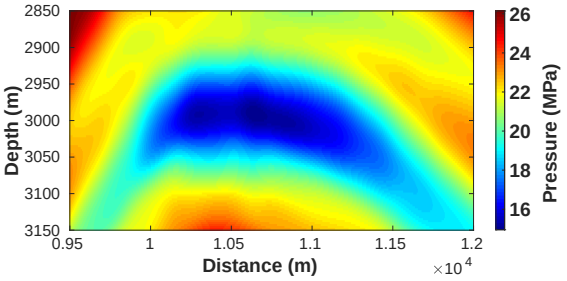

Figure 16: Complete solution with correction for normal horizontal stress, $\sigma_{xx}^{(c)} \approx \sigma_{xx}^{(h)} + \sigma_{xx}^{(p)} + \frac{1}{2}\sigma_{zz}^{(p)}$.

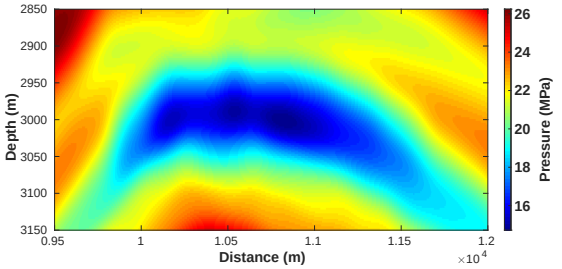

Figure 17: Normal horizontal stress from direct modeling, σ_{xx}.

Conclusions

The Marmousi model is characterized by the complexity of the input model, which includes the geometry of the geological structure and the distribution of physical parameters. An important question investigated in this experiment was whether the presence of gradients in velocity distributions can drastically change the solution. The Beltrami-Michell equation admits constant parameter values, and also isotropic, homogeneous, with smooth variations. In this experiment, our calculations were performed in the Marmousi model to measure the limitations of the method.

Poisson's coefficient (ν) is the main elastic parameter that affects the results of the Beltrami-Michell method. The presence of large velocity variations generates deviations in the expected values of the stress components. This work proposes a form of correction for these deviations based on the decomposition of the complete solution into homogeneous and particular solutions, bringing the results closer to those obtained by direct modeling.

This modeling should be analyzed on the geological scale, and not on the drilling engineering scale. The geological scale serves to characterize the geological basin, pointing towards a possible new reservoir site, or extending a productive reservoir. The methodology shows to be consistent in bringing out special details of the stress distribution, and the low and high-pressure zones that act as natural sucking pumps for oil and gas accumulation.

Acknowledgements

The authors would like to thank the Brazilian institution UFPA (*Universidade Federal do Pará*), the project National Institute of Science and Technology (INCT-GP, MCT/CNPq/FINEP).

References

Sadd, M. H. 2005. *Elasticity: Theory, Applications, and Numerics*, Oxford: Elsevier. 473 p.

Saada, A. S. 1974. *Elasticity Theory and Applications*, New York, NY, USA: Pergamon Press Inc. 643 p.

Novacky, V. *Theory of elasticity.*, Moscow: Mir. 872 p.

Fung, Y.C. 1965. *Foundations of Solid Mechanics*, London, England: Prentice-Hall, Inc.

Boresi, A.P.; Schmidt, R.F. 2003. *Advanced Mechanics of Materials*, New York, NY, USA: John Wiley and Sons, Inc. 611 p.

Polyanin, A. D.; Nazaikinskii, V. E. 2016. *Handbook of Linear Partial Differential Equations for Engineers and Scientists*, Boca Raton, FL, USA: CRC Press. 1623 p.

Martin, G.S.; Wiley, R.; Marfurt, K.J. 2006. Marmousi2: An elastic upgrade for marmousi. *The Leading Edge*, 25, 113-224.